



# Investigation of the antibacterial properties of silver nanoparticles synthesized using *Abelmoschus esculentus* extract and their ceramic applications

F. Elmusa<sup>1</sup> · A. Aygun<sup>1</sup> · F. Gulbagca<sup>1</sup> · A. Seyrankaya<sup>2</sup> · F. Gö<sup>3</sup> · C. Yenikaya<sup>4</sup> · F. Sen<sup>1</sup>

Received: 18 February 2020 / Revised: 1 July 2020 / Accepted: 30 July 2020 / Published online: 22 September 2020  
© Islamic Azad University (IAU) 2020

## Abstract

In this study, silver nanoparticles (Ag NPs) were successfully synthesized by using the green chemistry method, which is simple, environment friendly, and economical by using plant extract obtained from *Abelmoschus esculentus*. The synthesized Ag NPs were characterized using ultraviolet–visible (UV–Vis) spectroscopy, thermogravimetric analysis, transmission electron microscopy, Fourier transform infrared spectroscopy, X-ray crystallography and X-ray photoelectron spectroscopy. The synthesized Ag NPs showed absorbance peaks at 432 nm in the UV–Vis spectroscopy. The mean particle size of Ag NPs was found to be 8.96 nm. The antimicrobial activity of Ag NPs was examined on *Escherichia coli* (*E. coli*), *Staphylococcus aureus* (*S. aureus*), *Bacillus subtilis* (*B. subtilis*) and *Methicillin-resistant Staphylococcus aureus*. Besides, the antibacterial activity of Ag NPs was compared with commercially available antibiotics (Penicillin–streptomycin and Ampicillin–sulbactam). Ag NPs exhibited excellent antimicrobial activity against gram-positive and gram-negative bacteria. In addition, Ag NPs were used in ceramic glaze, and thus, an antibacterial ceramic glaze was developed.

**Keywords** *Abelmoschus esculentus* · Antimicrobial · Ceramic glaze · Green chemistry · Silver nanoparticles

## Introduction

Nanotechnology gained importance in scientific researches with the development of technology and led to the advancement of new materials in the nanoscale (Manoharan 2008).

In addition to the use of nanotechnology in chemistry, biology, physics, computers, electronics, and materials science, it also has a wide range of applications in medicines (Barkalina et al. 2014). Today, synthesized nanomaterials are used in areas such as gene therapy applications, orthopaedic applications, treatment of cardiological diseases, cancer treatment, and dental care (Misra et al. 2010). They are also used in the synthesis of safe, effective, and most importantly inexpensive and non-toxic drugs. Nanosize drugs have a specific effect, and they can spread to different areas in the body, and minimize the side effects (Farokhzad and Langer 2009). Drugs loaded with nanoparticles can increase biological activity by directly affecting diseased tissues and cells (Cho et al. 2008). Nanodrugs provide an advantage to them by eliminating small stature and immune responses and increase the ability to cross relatively impermeable membranes (Xia et al. 2019). Besides the production of these drugs, nanorobots with very small dimensions will be produced soon. These nanorobots can be injected into human blood to repair damaged organs in the human body (Ogawa et al. 2017). Also, blockages of brain capillaries can be eliminated with nanotubes. Accurate diagnosis and

Editorial responsibility: Samareh Mirkia.

**Electronic supplementary material** The online version of this article (<https://doi.org/10.1007/s13762-020-02883-x>) contains supplementary material, which is available to authorized users.

✉ F. Sen  
fatihsen1980@gmail.com

- <sup>1</sup> Sen Research Group, Department of Biochemistry, University of Dumlupinar, 43000 Kütahya, Turkey
- <sup>2</sup> Department of Mining Engineering, Faculty of Engineering, Dokuz Eylül University, Izmir, Turkey
- <sup>3</sup> Keramika Ceramics, Ünsa Mining, Tourism, Energy, Ceramics, Forest Products, Electricity Production Industry, Kutahya, Turkey
- <sup>4</sup> Department of Chemistry, Faculty of Science and Art, Dumlupinar University, Kutahya, Turkey

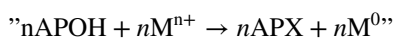


treatment can be made with nanotubes moving with blood in brain vessels (Saadeh and Vyas 2015).

Many types of nanoparticles have been successfully synthesized using metal ions (Li et al. 2007; Dubey et al. 2010a; Şahin et al. 2017; Aygun et al. 2019). In the literature, it has been reported that nanoporous and mesoporous metallic nanostructures are synthesized by soft- and hard-tempering methods (Ataee-Esfahani et al. 2011; Li et al. 2019). Nano-sized metallic particles are used for various purposes by varying their physical, chemical, and biological properties depending on their surface-volume ratios (Navya and Daima 2016). In the literature, different research groups have reported several method reviews on nanoparticle synthesis (Li et al. 2018a, b). Ag NPs, one of these nanoparticles, are gaining interest in various fields of application such as medicine, food, health, personal care, industry, optics, electricity, thermal, conductivity, and semi-conductivity due to their unique chemical and physical properties (Khan et al. 2017). Thanks to these properties, Ag NPs used in dressings, biological sensor technology, medical device coatings (Osuntokun and Onwudiwe 2018; Koskun et al. 2018; Najmeh Aboutorabi et al. 2019).

Various methods have also been adopted for the synthesis of Ag NPs with the highest yield, solubility, and stability (Dhand et al. 2015; Jayaprakash et al. 2019). In general, since traditional physical and chemical methods are very expensive and have problems, researchers adopted the biological methods as a simple, fast, non-toxic, and safe solution. In recent years, the “green chemistry” approach based on the synthesis of metal nanoparticles using plants and plant extracts has gained importance (Duan et al. 2015). Biomolecules such as terpenoids, alkaloids, phenolic compounds, enzymes, flavonoids, proteins, and polysaccharides present in the plant extract are involved in the reduction of metal salts. Biomolecules found in plant extract have a large impact on the size and distribution of metallic nanoparticles. Powerful reducing biomolecules in plant extract provide the synthesis of nanoparticles. Terpenoids, alkaloids, phenolic compounds, enzymes, flavonoids, proteins, and polysaccharides present in the plant extract function as capping agents and photo-components that provide stability to silver nanoparticles (Mittal et al. 2013; Küünaal et al. 2018). Polyphenols such as flavonoids are capable of H-donating and contain metal salts of sulfates, nitrates, and chlorides as powerful antioxidants in the reduction of metal precursors. The OH group in the reduced form of the polyphenolics is then converted into a carbonyl group by the reduction of metal ions due to a redox reaction. C=O groups in the oxidized form of polyphenol electrostatically stabilize metal nanoparticles (El-Seedi et al. 2019). Biomolecules in plant extract provide  $M^0$  reduction from  $M^+$ . The mechanism

of biosynthesis of metal salts is as follows (El-Seedi et al. 2019):



*Abelmoschus esculentus* (Okra), the only vegetable crop in the *Malvaceae* family, is an important and economic vegetable growing in tropical and tropical regions worldwide. Its main elements are K, Na, Mg, and Ca, and this plant has important antibacterial, antioxidant, antispasmodic activity (Duan et al. 2015). In this study, we aimed to synthesize Ag NPs by using green chemistry method using *A. esculentus* plant extract. UV–Vis, TEM, FTIR, TGA, XRD, and XPS analyses were performed for the characterization of synthesized nanoparticles. For the antibacterial activity of *A. esculentus* mediated Ag NPs, *E. coli*, *S. aureus*, *B. subtilis*, and *MRSA* strains were studied and the results were evaluated (Fig. 1).

## Materials and methods

### Materials

Analytical grade silver nitrate ( $\text{AgNO}_3$ ) and all the other chemicals used in this study were purchased from Sigma-Aldrich. Fresh *A. esculentus* (L.) was purchased from the local market.

### Extract of *Abelmoschus esculentus*

Fresh *A. esculentus* (L.) was ground in a mortar and pulped. 100 mL of 70% ethanol was added to 5 g of *A. esculentus* paste which was taken into 250-mL beaker. This mixture was heated to boiling in the microwave for 1 min (Tatke and Jaiswal 2011). This process was repeated until ethanol turned greenish color. The mixture was filtered through the filter paper. Subsequently, it was centrifuged at 7000 rpm. The obtained plant extract was stored at +4 °C for further experiments (Ravichandran et al. 2019).

### Synthesis of silver nanoparticles

The different concentration of silver nitrate solution (0.5, 1, 3 and 5 mM) was added to the *A. esculentus* (L.) extract (1, 3, 5 and 10 mL) taken in a round bottom flask to bring the final volume to 100 mL (Sahni et al. 2015; Sana and Dogiparthi 2018). The round bottom flask containing the sample was kept under reflux (25, 50, 75, and 100 °C) until the reaction was completed, and the mixture turned dark. UV–Vis absorbance values were measured at specific time intervals (0, 6, 12, and 24 h). The dark-colored extract mixture was



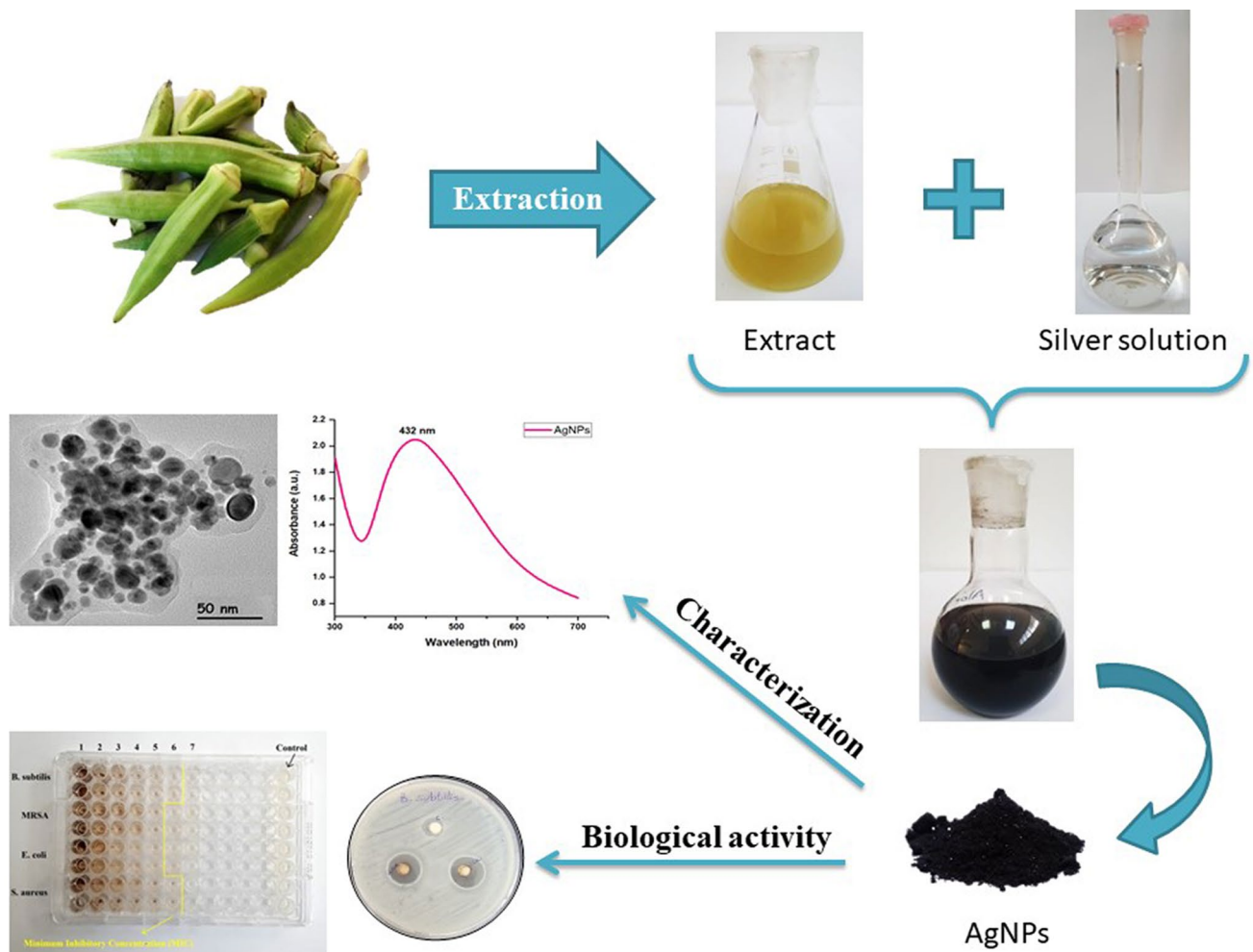


**Fig. 1** Schematic representation of the synthesis of Ag NPs by green chemistry method using *A. esculentus* extract

washed several times with 90% ethanol until the supernatant was clear. The washed Ag NPs were poured into a petri dish and dried in an oven. Obtained particles were stored in an Eppendorf tube at room temperature.

## Characterization

### UV–Vis absorption spectroscopy

The formation of Ag NPs was controlled by UV–Vis spectrometer (Lambda 750 UV/VIS/NIR) at a wavelength range from 300 to 700 nm.

### Transmission electron microscopy (TEM)

TEM was used for the analysis of synthesized Ag NPs morphology. The poured sample suspension on a carbon-coated copper grid was dried overnight at room temperature. The

TEM analysis was performed in the JEM JEOL 2100 F at an acceleration voltage of 200 kV.

### X-ray diffraction (XRD)

The crystal structure of Ag NPs synthesized by green chemistry method was confirmed by XRD analysis. For this purpose, the solid Ag NPs were analyzed in the 20°–90° range with a 40 kV voltage using the Rigaku Ultima-IV X-ray diffraction device with CuK $\alpha$  radiation.

### X-ray photoelectron spectroscopy (XPS)

X-ray photoelectron spectroscopy was used to elucidate the chemical status and near-surface composition of *A. esculentus* (L.) mediated Ag NPs. The scanning spectra of the sample surface were analyzed with the PHI 5000 VersaProbe instrument.

## Fourier transform infrared (FTIR) spectroscopy

FTIR analysis was performed to determine the functional groups of biomolecules in plant extracts which were responsible for the reduction of  $\text{Ag}^+$  ions and stabilization of Ag NPs. FTIR analysis of nanoparticles was performed with Spectrum Two FTIR spectrometer at  $4\text{ cm}^{-1}$  resolution in the range of  $4000\text{--}400\text{ cm}^{-1}$ .

## Thermogravimetric analysis

Thermogravimetry is generally used to determine mass loss and/or gains in materials as a function of temperature or time. PerkinElmer Pyris 1 device was used for TGA analysis.

## Antimicrobial assay

### Disk diffusion assay

The disk diffusion method was used to investigate the antibacterial activity of Ag NPs. For this, single colony bacterial suspension was inoculated into nutrient agar. After pipetting Ag NPs (concentration  $200\text{ }\mu\text{g/mL}$  and  $100\text{ }\mu\text{g/mL}$ ) onto 6-mm sterile paper disks, the inoculated agar was placed on the surface (Balouiri et al. 2016). Negative control was used as plant aqueous extract on the surface of each plate. Two commercial antibiotics, Penicillin–streptomycin (PS) ( $10,000\text{ U} + 10\text{ mg}$ ) and Ampicillin–sulbactam (AS) were also tested as positive controls on the surface of a separate plate. Plates were then incubated at  $37\text{ }^\circ\text{C}$  for 24 h. The diameters of zones were measured and compared (Farzana et al. 2017). In addition, two different concentrations of Ag NPs were added into the ceramic glaze and tested with the same procedure.

### Minimum inhibitory concentration (MIC) and minimum bactericidal concentration (MBC) test

The MIC of the synthesized Ag NPs was determined by a two-layer serial dilution method. Ag NPs dissolved in DMSO were diluted to concentrations of 200, 100, 50, 25, 12.5, 6.25, and  $3.125\text{ }\mu\text{g/mL}$ , and a 24-h fresh bacterial suspension prepared the day before was added according to the 0.5 McFarland constant. The microplates were incubated at  $37\text{ }^\circ\text{C}$  for 24 h. The macroscopic evaluation of the wells that did not observe the growth of the organism was then determined as the MIC (Farzana et al. 2017).

Microscopic wells without bacterial growth were added to sterile agar plates and incubated for 24 h ( $37\text{ }^\circ\text{C}$ ). After the incubation period, wells that did not allow bacterial

colonies to grow were recorded as MBC values (Olajuyigbe and Afolayan 2012).

## Results and discussion

### UV–Vis absorption spectroscopy analysis

Figure 2 shows the absorbance spectrum of Ag NPs (synthesized using  $1\text{ mM AgNO}_3$  and  $10\text{ mL}$  plant extract) after 48 h at room temperature. The absorbance spectrum of Ag NPs showed an absorbance band at approximately  $432\text{ nm}$  as shown in Fig. 2. Results were consistent with the literature (Jayaprakash et al. 2017; Fatimah and Indriani 2018; Aygün et al. 2019; Vyas et al. 2019). The effect of different concentrations of  $\text{AgNO}_3$  salt ( $0.5, 1, 3,$  and  $5\text{ mM}$ ) against the synthesis of Ag NPs in  $5\text{ mL}$  of plant extract was examined for 1 h at  $75\text{ }^\circ\text{C}$  (Fig. 3a). In the spectrum, it was observed that with the increase of  $\text{AgNO}_3$  salt concentration, the reduction of  $\text{Ag}^+$  to  $\text{Ag}^0$  was increased, and as a result of this, the peak density increased (Kolya et al. 2015; Miri et al. 2018). Figure 3b shows the effect of different amounts of aqueous extract volumes on the synthesis of Ag NPs. The shifting of the plasmon resonance peak toward higher wavelengths with increasing plant extract volumes indicates that a decrease in the particle size of Ag NPs occurs (Dubey et al. 2010b; Balashanmugam et al. 2016; Kahsay et al. 2018; Samari et al. 2019). Figure 3c shows the effect of different reaction temperatures ( $25, 50, 75,$  and  $100\text{ }^\circ\text{C}$ ) on the synthesis of Ag NPs ( $5\text{ mM AgNO}_3, 5\text{ mL}$  extract, and 1 h). With increasing reaction temperature, an increase in peak intensity and a

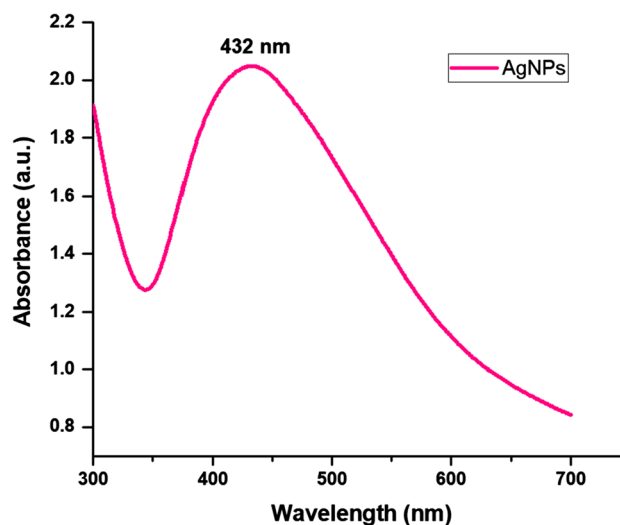
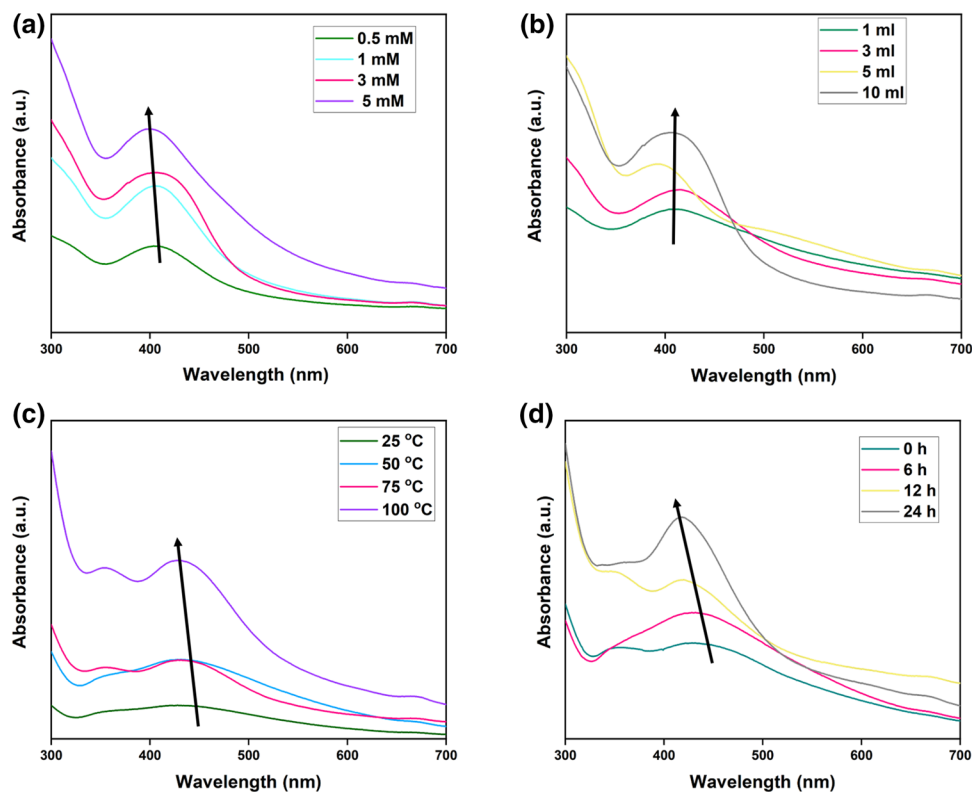


Fig. 2 UV–Vis analysis of Ag NPs synthesized by the green chemistry method using *A. esculentus* extract

**Fig. 3** UV–Vis spectra of Ag NPs at **a** different concentrations of  $\text{AgNO}_3$ , **b** different volumes of the extract of *A. esculentus*, **c** different temperatures and **d** different reaction times



shift toward low wavelengths are observed. This means that more nanoparticles are synthesized or the size of the nanoparticles decreases (Gavade et al. 2015; Ndikau et al. 2017). Figure 3d shows the effects of different reaction times (0, 6, 12, and 24 h) on the synthesis of Ag NPs (5 mM  $\text{AgNO}_3$ , 5 mL extract, and 75 °C). It is seen that as the reaction times increase, the resulting peaks become stronger. Also, as the reaction time increases, the shifts in the peaks indicate the reduced size of Ag NPs (Mashrai et al. 2018; Zafar and Zafar 2019).

### X-ray diffraction (XRD) analysis

The crystal structure of Ag NPs synthesized using *A. esculentus* (L.) plant extract was determined by XRD analysis. As shown in Fig. 4, peaks of 38.11°, 44.22°, 64.35°, 77.33° and 81.14° were observed corresponding to the lattice planes (111), (200), (220), (311) and (322), respectively (Mostafa et al. 2015; Panja et al. 2016). The average crystalline size

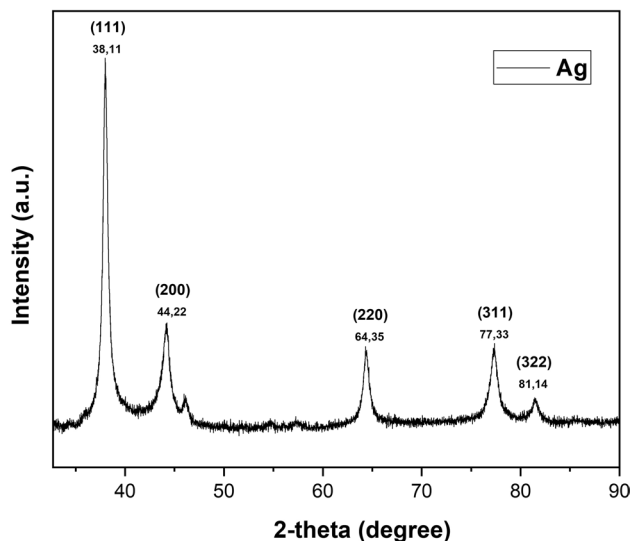


**Fig. 4** XRD image of Ag NPs synthesized by green chemistry method using *A. esculentus* extract

of Ag NPs was calculated using the Debye–Scherrer formula and was found to be 11.51 nm. It was observed that the results of this study were compatible with the XRD results in the literature.

### X-ray photoelectron spectroscopy (XPS) analysis

In the XPS image of Ag NPs (Fig. 5), Ag  $3d_{5/2}$  and Ag  $3d_{3/2}$  peaks can be divided into two peak pairs, respectively, at 366.5 and 372.7 eV which confirming the presence of silver nanoparticles (Chairam and Somsook 2016; Quites et al. 2017; Sharma et al. 2018).

### Transmission electron microscopy (TEM) analysis

The morphology, mean particle size, and shape of Ag NPs synthesized using plant extract were determined by TEM

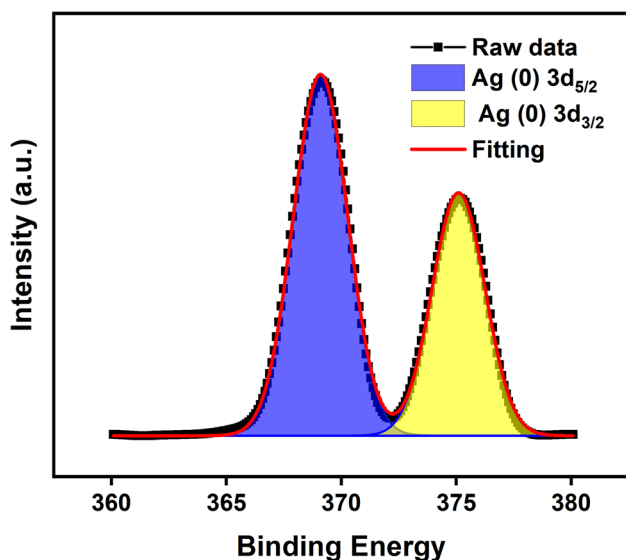
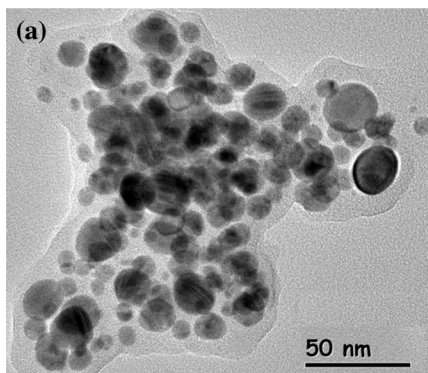


**Fig. 5** XPS analysis of Ag NPs synthesized by green chemistry method using *A. esculentus* extract

**Fig. 6** **a** TEM image, **b** particle size histogram of Ag NPs synthesized by green chemistry method using *A. esculentus* extract



(Hamouda et al. 2019). The TEM image of the synthesized Ag NPs is shown in Fig. 6a; it was observed that the particles did not contain any agglomeration and consisted of spherical particles. The particle size of Ag NPs was calculated to be 8.96 nm on average (Fig. 6b). The particle distribution was observed that most of the joints ranged from 4 to 15 nm.

### Fourier transform infrared (FTIR) spectroscopy analysis

The FTIR spectrum of Ag NPs synthesized using *A. esculentus* (L.) extract contains a plurality of characteristic bands as shown in Fig. 7. The peak of  $3260\text{ cm}^{-1}$  in the spectrum of *A. esculentus* (L.) extract corresponds to the stress and bending vibrations of N–H bonds in amines from proteins in plants and O–H bonds in alcohols (Zia et al. 2016). The peak at  $2979\text{ cm}^{-1}$  is responsible for the stretching vibration of the  $\text{CH}_3$  groups. The peak at  $1635\text{ cm}^{-1}$  belongs to the amide I protein group. The peak at  $1044\text{ cm}^{-1}$  results

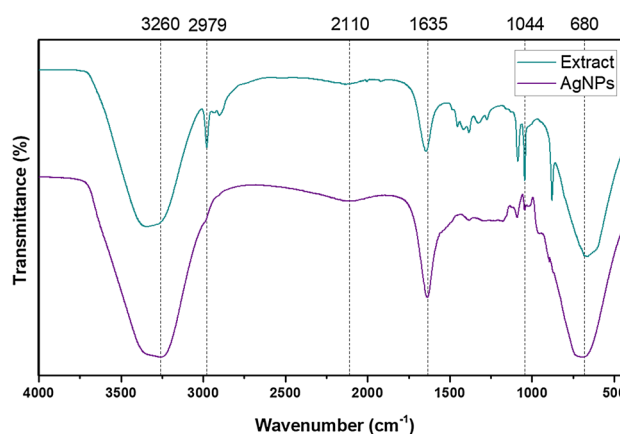


**Fig. 7** FTIR analysis of Ag NPs synthesized by green chemistry method using *A. esculentus* extract





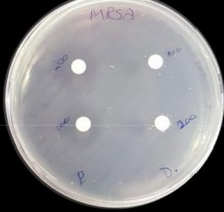



from the C–O–C group antisymmetric tensile vibrations of polysaccharides (Mollick et al. 2015; Abraham et al. 2017). Finally, the peak at  $680\text{ cm}^{-1}$  corresponds to C–H flexion, which proves the presence of aromatic compounds. These FTIR peaks clearly show the presence of proteins, terpenoids, and flavonoids in the aqueous extract of *A. esculentus* (L.) (AbuDalo et al. 2019). According to the FTIR spectrum of Ag NPs synthesized from *A. esculentus* (L.) extract, the peaks of the plant extract are similar with a slight shift. This indicates that *A. esculentus* (L.) extract is reduced by metal ions and plays an important role in the stabilization of nanoparticles. The flavonoids and terpenoids contained in the plant extracts play a role in the reduction of silver metals and the synthesis of Ag NPs, while proteins have stabilized the nanoparticles synthesized by coating them around Ag NPs (Singh et al. 2018).

## Thermogravimetric analysis

TGA and DTA results show that the first gradual weight loss around  $100\text{ }^{\circ}\text{C}$  is due to the moisture adsorbed on the surface. The first significant weight loss at  $259\text{ }^{\circ}\text{C}$  is related to the evaporation of organic content which doped on Ag particles. The second weight-loss step is also related to the desorption of bioorganic compounds, which has higher boiling points, from plant extract.

Since the weight of the Ag NPs is not changed by the temperature increase, weight loss indicates the existence of organic compounds on the Ag surface. Therefore, we can conclude that organic compound doped on the Ag NPs is around 35%. Also, TGA analysis proves that biosynthesized Ag NPs are applicable up to  $200\text{ }^{\circ}\text{C}$  (Figure S1).

**Table 1** Zone diameters of Ag NPs synthesized by the green chemistry method using *A. esculentus* extract

	Zone of inhibition (mm)	Antibiotics	Ag NPs
<i>S. aureus</i>	Control (water): 0 PS (100 $\mu\text{g/ml}$ ): 35 AS (100 $\mu\text{g/ml}$ ): 28		
	Control (extract): 10 Ag NPs (100 $\mu\text{g/ml}$ ): 18 Ag NPs (200 $\mu\text{g/ml}$ ): 20		
<i>E. coli</i>	Control (water): 0 PS (100 $\mu\text{g/ml}$ ): 20 AS (100 $\mu\text{g/ml}$ ): 10		
	Control (extract): 11 Ag NPs (100 $\mu\text{g/ml}$ ): 17 Ag NPs (200 $\mu\text{g/ml}$ ): 18		
MRSA	Control (water): 0 PS (100 $\mu\text{g/ml}$ ): 12 AS (100 $\mu\text{g/ml}$ ): 0		
	Control (extract): 0 Ag NPs (100 $\mu\text{g/ml}$ ): 16 Ag NPs (200 $\mu\text{g/ml}$ ): 20		
<i>B. subtilis</i>	Control (water): 0 PS (100 $\mu\text{g/ml}$ ): 20 AS (100 $\mu\text{g/ml}$ ): 18		
	Control (extract): 10 Ag NPs (100 $\mu\text{g/ml}$ ): 16 Ag NPs (200 $\mu\text{g/ml}$ ): 17		

## Antimicrobial activity of silver nanoparticles against microorganisms

Ag NPs showed high antibacterial activity against *B. subtilis*, *E. coli*, *S. Aureus*, and *MRSA*. The diameters obtained from Ag NPs at the concentration of 200  $\mu\text{g}/\text{mL}$  by disk diffusion method are 17, 18, 20, and 20 mm, respectively. Ag NPs at a concentration of 100  $\mu\text{g}/\text{mL}$  obtained 16, 17, 18, and 16 mm values (Nanda and Saravanan 2009; Arul et al. 2017; Qais et al. 2019). When clear regions (zone diameters) from Ag NPs synthesized as shown in Table 1 are compared to commercial antibiotics, zone diameters of Ag NPs are very close. The reason is that commercial antibiotics used are thought to be from a mixture of two strong antibiotics. However, Ag NPs seem to limit bacterial growth better than commercial antibiotics against *MRSA* bacteria and have higher antibacterial activity.

Ag NPs examined by the Dilution Method on *B. subtilis*, *E. coli*, *S. aureus*, and *MRSA* bacteria showed 77, 74, 72, and 67% inhibition, respectively, at 200  $\mu\text{g}/\text{mL}$  concentration as shown in Fig. 8. Proportional results were obtained depending on the concentration of Ag NPs.

In addition, MIC and MBC values of all tested bacterial strains were determined as shown in Fig. 9. The recorded MIC and MBC values are shown in Table 2 (Omara et al. 2017; Loo et al. 2018).

Finally, the results of antimicrobial ceramic glaze development were obtained as shown in Table 3. Ceramic glaze containing Ag NPs (100  $\mu\text{g}/\text{mL}$ ), respectively, produced

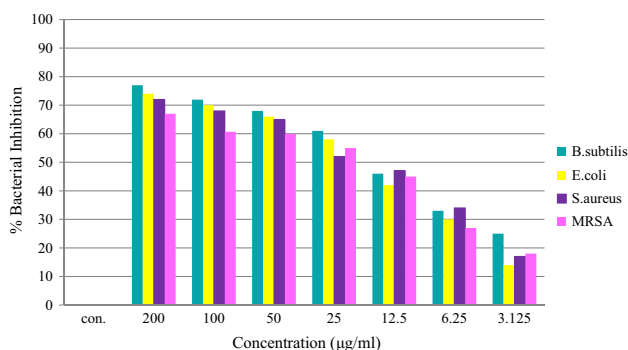


**Fig. 8** %Bacterial inhibition of Ag NPs synthesized by the green chemistry method using *A. esculentus* extract

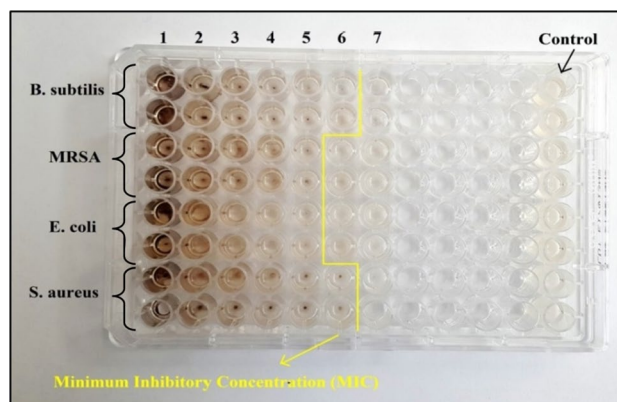


**Fig. 9** Microplate image of microbroth dilution test result of Ag NPs synthesized by green chemistry method using *A. esculentus* extract

**Table 2** Microplate image of microbroth dilution test result of Ag NPs synthesized by green chemistry method using *A. esculentus* extract

Bacteria	MIC ( $\mu\text{g}/\text{mL}$ )	MBC ( $\mu\text{g}/\text{mL}$ )
<i>B. subtilis</i>	6.25	6.25
<i>MRSA</i>	12.5	25
<i>E. coli</i>	12.5	12.5
<i>S. aureus</i>	6.25	12.5

zone diameters of 22, 18, 17, and 20 mm against *S. aureus*, *E. coli*, *MRSA*, and *B. subtilis* bacterias.





## Conclusion

The synthesis of small size Ag NPs using *A. esculentus* (L.) extract was carried out by the green chemistry method, which is environmentally friendly and cost-effective. The formation of Ag NPs was confirmed by FTIR, UV–Vis, TGA, TEM, XRD, and XPS. The TEM analysis result showed that the synthesized Ag NPs were stable with an average size of 8.96 nm. The particle size calculated as a result of XRD analysis supports the TEM analysis result. TGA results showed that approximately 35% of organic





**Table 3** Zone diameters of antibacterial ceramic glaze with Ag NP synthesized by green chemistry method using *A. esculentus* extract

	Zone of inhibition (mm)	Ag NPs
<i>S. aureus</i>	Control: 0 Ceramic glaze (50 $\mu\text{g/ml}$ Ag NPs): 20 Ceramic glaze (100 $\mu\text{g/ml}$ Ag NPs): 22	
<i>E. coli</i>	Control: 0 Ceramic glaze (50 $\mu\text{g/ml}$ Ag NPs): 15 Ceramic glaze (100 $\mu\text{g/ml}$ Ag NPs): 18	
<i>MRSA</i>	Control: 0 Ceramic glaze (50 $\mu\text{g/ml}$ Ag NPs): 15 Ceramic glaze (100 $\mu\text{g/ml}$ Ag NPs): 17	
<i>B. subtilis</i>	Control: 0 Ceramic glaze (50 $\mu\text{g/ml}$ Ag NPs): 16 Ceramic glaze (100 $\mu\text{g/ml}$ Ag NPs): 20	

compounds from plant extract was doped on as-synthesized Ag NPs. Ag NPs investigated for their biological activity on *B. subtilis*, *E. coli*, *S. Aureus* and *MRSA* bacterial strains proved to have a very good antimicrobial activity compared to commercial antibiotics, and their effect on *MRSA* bacteria was greater than that of commercial antibiotics. Also, Ag NPs added to the ceramic glaze structure were observed to have high antibacterial activity. It is considered that molecular studies should be carried out to understand this in future studies. Furthermore, according to the data obtained in this study, Ag NPs can be a promising candidate for medical and biomedical applications.

**Acknowledgement** The authors would like to thank Keramika Ceramics Company, Kutahya, Turkey.

### Compliance with ethical standards

**Conflict of interest** The authors declare that they have no conflict of interest.

### References

Aboutorabi SN, Nasiriboroumand M, Mohammadi P, Sheibani H, Barani H (2019) Preparation of antibacterial cotton wound dressing by green synthesis silver nanoparticles using mullein leaves

- extract. *J Renew Mater* 7:787–794. <https://doi.org/10.32604/jrm.2019.06438>
- Abraham J, Saraf S, Mustafa V, Chaudhary Y, Sivanangam S (2017) Synthesis and evaluation of silver nanoparticles using *Cymodocea rotundata* against clinical pathogens and human osteosarcoma cell line. *J Appl Pharm Sci* 7:055–061. <https://doi.org/10.7324/japs.2017.70608>
- AbuDalo MA, Al-Mheidat IR, Al-Shurafat AW, Grinham C, Oyanedel-Craver V (2019) Synthesis of silver nanoparticles using a modified Tollens' method in conjunction with phytochemicals and assessment of their antimicrobial activity. *PeerJ*. <https://doi.org/10.7717/peerj.6413>
- Arul D, Balasubramani G, Balasubramanian V, Natarajan T, Perumal P (2017) Antibacterial efficacy of silver nanoparticles and ethyl acetate's metabolites of the potent halophilic (marine) bacterium, *Bacillus cereus* A30 on multidrug resistant bacteria. *Pathog Glob Health* 111:367–382. <https://doi.org/10.1080/20477724.2017.1390829>
- Ataee-Esfahani H, Nemoto Y, Wang L, Yamauchi Y (2011) Rational synthesis of Pt spheres with hollow interior and nanosponge shell using silica particles as template. *Chem Commun* 47:3885–3887. <https://doi.org/10.1039/c0cc05233g>
- Aygun A, Gülbagca F, Ozer LY et al (2019) Biogenic platinum nanoparticles using black cumin seed and their potential usage as antimicrobial and anticancer agent. *J Pharm Biomed Anal* 179:112961–112969. <https://doi.org/10.1016/j.jpba.2019.112961>
- Aygun A, Özdemir S, Gülcan M, Cellat K, Şen F (2019) Synthesis and characterization of Reishi mushroom-mediated green synthesis of silver nanoparticles for the biochemical applications. *J Pharm Biomed Anal* 178:112970–112977. <https://doi.org/10.1016/j.jpba.2019.112970>
- Balashanmugam P, Balakumaran MD, Murugan R, Dhanapal K, Kalai-chelvan PT (2016) Phytochemical synthesis of silver nanoparticles, optimization and evaluation of in vitro antifungal activity against human and plant pathogens. *Microbiol Res* 192:52–64. <https://doi.org/10.1016/j.micres.2016.06.004>
- Balouiri M, Sadiki M, Ibsouda SK (2016) Methods for in vitro evaluating antimicrobial activity: a review. *J Pharm Anal* 6:71–79. <https://doi.org/10.1016/j.jpba.2015.11.005>
- Barkalina N, Charalambous C, Jones C, Coward K (2014) Nanotechnology in reproductive medicine: emerging applications of nanomaterials. *Nanomed Nanotechnol Biol Med* 10:e921–e938. <https://doi.org/10.1016/j.nano.2014.01.001>
- Chairam S, Somsook E (2016) Facile, versatile and green synthesis of silver nanoparticles by mung bean starch and their catalytic activity in the reduction of 4-nitrophenol. *Chiang Mai J Sci* 43:609–619
- Cho K, Wang X, Nie S, Chen Z, Shin DM (2008) Therapeutic nanoparticles for drug delivery in cancer. *Clin Cancer Res* 14:1310–1316. <https://doi.org/10.1158/1078-0432.ccr-07-1441>
- Dhand C, Dwivedi N, Loh XJ et al (2015) Methods and strategies for the synthesis of diverse nanoparticles and their applications: a comprehensive overview. *RSC Adv* 5:105003–105037
- Duan H, Wang D, Li Y (2015) Green chemistry for nanoparticle synthesis. *Chem Soc Rev* 44:5778–5792. <https://doi.org/10.1039/c4cs00363b>
- Dubey SP, Lahtinen M, Sillanpää M (2010a) Green synthesis and characterizations of silver and gold nanoparticles using leaf extract of *Rosa rugosa*. *Colloids Surfaces A Physicochem Eng Asp* 364:34–41. <https://doi.org/10.1016/j.colsurfa.2010.04.023>
- Dubey SP, Lahtinen M, Sillanpää M (2010b) Tansy fruit mediated greener synthesis of silver and gold nanoparticles. *Process Biochem* 45:1065–1071. <https://doi.org/10.1016/j.procbio.2010.03.024>
- El-Seedi HR, El-Shabasy RM, Khalifa SAM et al (2019) Metal nanoparticles fabricated by green chemistry using natural extracts: biosynthesis, mechanisms, and applications. *RSC Adv* 9:24539–24559
- Farokhzad OC, Langer R (2009) Impact of nanotechnology on drug delivery. *ACS Nano* 3:16–20. <https://doi.org/10.1021/nn900002m>
- Farzana R, Iqra P, Shafaq F et al (2017) Antimicrobial behavior of zinc oxide nanoparticles and  $\beta$ -lactam antibiotics against pathogenic bacteria. *Arch Clin Microbiol* 08:57. <https://doi.org/10.4172/1989-8436.100057>
- Fatimah I, Indriani N (2018) Silver nanoparticles synthesized using Lantana Camara flower extract by Reflux, microwave and ultrasound methods. *Chem J Mold* 13:95–102. <https://doi.org/10.19261/cjm.2017.461>
- Gavade SJM, Nikam GH, Dhabbe RS, Sabale SR, Tamhankar BV, Mulik GN (2015) Green synthesis of silver nanoparticles by using carambola fruit extract and their antibacterial activity. *Adv Nat Sci Nanosci Nanotechnol* 6:045015–045021. <https://doi.org/10.1088/2043-6262/6/4/045015>
- Hamouda RA, Hussein MH, Abo-elmagd RA, Bawazir SS (2019) Synthesis and biological characterization of silver nanoparticles derived from the cyanobacterium *Oscillatoria limnetica*. *Sci Rep* 9:13071–13088. <https://doi.org/10.1038/s41598-019-49444-y>
- Jayaprakash N, Vijaya JJ, Kaviyarasu K et al (2017) Green synthesis of Ag nanoparticles using Tamarind fruit extract for the antibacterial studies. *J Photochem Photobiol B Biol* 169:178–185. <https://doi.org/10.1016/j.jphotobiol.2017.03.013>
- Jayaprakash N, Suresh R, Rajalakshmi S et al (2019) An assortment of synthesis methods of silver nanoparticles: a review. *Asian J Chem* 31:1405–1412. <https://doi.org/10.14233/ajchem.2019.21972>
- Kahsay MH, RamaDevi D, Kumar YP, Mohan BS, Tadesse A, Battu G, Basavaiah K (2018) Synthesis of silver nanoparticles using aqueous extract of Dolichos lablab for reduction of 4-Nitrophenol, antimicrobial and anticancer activities. *OpenNano* 3:28–37. <https://doi.org/10.1016/j.onano.2018.04.001>
- Khan I, Saeed K, Khan I (2017) Nanoparticles: properties, applications and toxicities. *Arab J Chem*. <https://doi.org/10.1016/j.arabj.2017.05.011>
- Kolya H, Maiti P, Pandey A, Tripathy T (2015) Green synthesis of silver nanoparticles with antimicrobial and azo dye (Congo red) degradation properties using *Amaranthus gangeticus* Linn leaf extract. *J Anal Sci Technol* 6:1–7. <https://doi.org/10.1186/s40543-015-0074-1>
- Koskun Y, Şavk A, Şen B, Şen F (2018) Highly sensitive glucose sensor based on monodisperse palladium nickel/activated carbon nanocomposites. *Anal Chim Acta* 1010:37–43. <https://doi.org/10.1016/j.aca.2018.01.035>
- Küünl S, Rauwel P, Rauwel E (2018) Plant extract mediated synthesis of nanoparticles. In: Emerging applications of nanoparticles and architectural nanostructures: current prospects and future trends. Elsevier, Amsterdam, pp 411–446
- Li S, Shen Y, Xie A, Yu X, Qiu L, Zhang L, Zhang Q (2007) Green synthesis of silver nanoparticles using *Capsicum annum* L. extract. *Green Chem* 9:852–858. <https://doi.org/10.1039/b615357g>
- Li C, Iqbal M, Lin J et al (2018a) Electrochemical deposition: an advanced approach for templated synthesis of nanoporous metal architectures. *Acc Chem Res* 51:1764–1773. <https://doi.org/10.1021/acs.accounts.8b00119>

- Li C, Tan H, Lin J et al (2018b) Emerging Pt-based electrocatalysts with highly open nanoarchitectures for boosting oxygen reduction reaction. *Nano Today* 21:91–105. <https://doi.org/10.1016/j.nantod.2018.06.005>
- Li C, Iqbal M, Jiang B et al (2019) Pore-tuning to boost the electrocatalytic activity of polymeric micelle-templated mesoporous Pd nanoparticles. *Chem Sci* 10:4054–4061. <https://doi.org/10.1039/c8sc03911a>
- Loo YY, Rukayadi Y, Nor-Khaizura MAR, Kuan CH, Chieng BW, Nishibuchi M, Radu S (2018) In Vitro antimicrobial activity of green synthesized silver nanoparticles against selected Gram-negative foodborne pathogens. *Front Microbiol* 9:1555–1562. <https://doi.org/10.3389/fmicb.2018.01555>
- Manoharan M (2008) Research on the frontiers of materials science: the impact of nanotechnology on new material development. *Technol Soc* 30:401–404. <https://doi.org/10.1016/j.techsoc.2008.04.016>
- Mashrai A, Mahmood Dar A, Asif Sherwani M, Singh BR (2018) Biosynthesis of silver nanoparticles as a platform for biomedical application. *J Nanosci Nanomed* 2:25–33
- Miri A, Mousavi SR, Sarani M, Mahmoodi Z (2018) Using Biebersteinia multifida aqueous extract, and the photocatalytic activity of synthesized silver nanoparticles. *Orient J Chem* 34:1513–1517. <https://doi.org/10.13005/ojc/340342>
- Misra R, Acharya S, Sahoo SK (2010) Cancer nanotechnology: application of nanotechnology in cancer therapy. *Drug Discov Today* 15:842–850. <https://doi.org/10.1016/j.drudis.2010.08.006>
- Mittal AK, Chisti Y, Banerjee UC (2013) Synthesis of metallic nanoparticles using plant extracts. *Biotechnol Adv* 31:346–356
- Mollick MMR, Rana D, Dash SK et al (2015) Studies on green synthesized silver nanoparticles using *Abelmoschus esculentus* (L.) pulp extract having anticancer (in vitro) and antimicrobial applications. *Arab J Chem* 12:2572–2584. <https://doi.org/10.1016/j.arabjc.2015.04.033>
- Mostafa AA, Sayed SRM, Solkamy EN et al (2015) Evaluation of biological activities of chemically synthesized silver nanoparticles. *J Nanomater* 2015:789178–789185. <https://doi.org/10.1155/2015/789178>
- Nanda A, Saravanan M (2009) Biosynthesis of silver nanoparticles from *Staphylococcus aureus* and its antimicrobial activity against MRSA and MRSE. *Nanomed Nanotechnol Biol Med* 5:452–456. <https://doi.org/10.1016/j.nano.2009.01.012>
- Navya PN, Daima HK (2016) Rational engineering of physicochemical properties of nanomaterials for biomedical applications with nanotoxicological perspectives. *Nano Converg*. <https://doi.org/10.1186/s40580-016-0064-z>
- Ndikau M, Noah NM, Andala DM, Masika E (2017) Green synthesis and characterization of silver nanoparticles using *Citrullus lanatus* fruit rind extract. *Int J Anal Chem*. <https://doi.org/10.1155/2017/8108504>
- Ogawa K, Uesugi K, Morishima K (2017) On-chip internalization process of an intracellular nanobot into a single cell. In: Proceedings of the IEEE international conference on micro electro mechanical systems (MEMS)
- Olajuyigbe OO, Afolayan AJ (2012) In Vitro antibacterial and time-kill evaluation of the *Erythrina caffra* thub. Extract against bacteria associated with diarrhoea. *Sci World J* 2012:738314–738322. <https://doi.org/10.1100/2012/738314>
- Omara ST, Zawrah MF, Samy AA (2017) Minimum bactericidal concentration of chemically synthesized silver nanoparticles against pathogenic Salmonella and Shigella strains isolated from layer poultry farms. *J Appl Pharm Sci* 7:214–221. <https://doi.org/10.7324/japs.2017.70829>
- Osuntokun J, Onwudiwe DC (2018) Phyto-mediated synthesis and photocatalytic activity of nanoparticles using aqueous extract of broccoli. *Nano Res Appl* 4:44. <https://doi.org/10.21767/2471-9838-c2-012>
- Panja S, Chaudhuri I, Khanra K, Bhattacharyya N (2016) Biological application of green silver nanoparticle synthesized from leaf extract of *Rauwolfia serpentina* Benth. *Asian Pac J Trop Dis* 6:549–556. [https://doi.org/10.1016/s2222-1808\(16\)61085-x](https://doi.org/10.1016/s2222-1808(16)61085-x)
- Qais FA, Shafiq A, Khan HM et al (2019) Antibacterial effect of silver nanoparticles synthesized using *Murraya koenigii* (L.) against multidrug-resistant pathogens. *Bioinorg Chem Appl* 2019:1–11. <https://doi.org/10.1155/2019/4649506>
- Quites F, Azevedo CKS, Alves EPP et al (2017) Ag nanoparticles-based zinc hydroxide-layered hybrids as novel and efficient catalysts for reduction of 4-nitrophenol to 4-aminophenol. *J Braz Chem Soc* 28:106–115. <https://doi.org/10.5935/0103-5053.20160152>
- Ravichandran V, Vasanthi S, Shalini S et al (2019) Green synthesis, characterization, antibacterial, antioxidant and photocatalytic activity of *Parkia speciosa* leaves extract mediated silver nanoparticles. *Results Phys* 15:102565. <https://doi.org/10.1016/j.rinp.2019.102565>
- Saaddeh Y, Vyas D (2015) Nanorobotic applications in medicine: current proposals and designs. *Am J Robot Surg* 1:4–11. <https://doi.org/10.1166/ajrs.2014.1010>
- Şahin B, Demir E, Aygün A, Gündüz H, Şen F (2017) Investigation of the effect of pomegranate extract and monodisperse silver nanoparticle combination on MCF-7 cell line. *J Biotechnol* 260:79–83. <https://doi.org/10.1016/j.jbiotec.2017.09.012>
- Sahni G, Panwar A, Kaur B (2015) Controlled green synthesis of silver nanoparticles by *Allium cepa* and *Musa acuminata* with strong antimicrobial activity. *Int Nano Lett* 5:93–100. <https://doi.org/10.1007/s40089-015-0142-y>
- Samari F, Parkhari P, Eftekhari E et al (2019) Antioxidant, cytotoxic and catalytic degradation efficiency of controllable phyto-synthesized silver nanoparticles with high stability using *Cordia myxa* extract. *J Exp Nanosci* 14:141–159. <https://doi.org/10.1080/107458080.2019.1687883>
- Sana SS, Dogiparthi LK (2018) Green synthesis of silver nanoparticles using *Givotia moluccana* leaf extract and evaluation of their antimicrobial activity. *Mater Lett* 226:47–51. <https://doi.org/10.1016/j.matlet.2018.05.009>
- Sharma R, Dhillion A, Kumar D (2018) Mentha-stabilized silver nanoparticles for high-performance colorimetric detection of Al(III) in aqueous systems. *Sci Rep* 8:5189–5202. <https://doi.org/10.1038/s41598-018-23469-1>
- Singh J, Dutta T, Kim KH et al (2018) “Green” synthesis of metals and their oxide nanoparticles: applications for environmental remediation. *J Nanobiotechnol* 16:84
- Tatke P, Jaiswal Y (2011) An overview of microwave assisted extraction and its applications in herbal drug research. *Res J Med Plant* 5:21–31. <https://doi.org/10.3923/rjmp.2011.21.31>
- Vyas G, Bhatt S, Paul P (2019) Synthesis of calixarene-capped silver nanoparticles for colorimetric and amperometric detection of mercury (Hg II, Hg 0). *ACS Omega* 4:3860–3870. <https://doi.org/10.1021/acsomega.8b03299>
- Xia Q, Zhang Y, Li Z et al (2019) Red blood cell membrane-camouflaged nanoparticles: a novel drug delivery system for



- antitumor application. *Acta Pharm Sin B* 9:675–689. <https://doi.org/10.1016/j.apsb.2019.01.011>
- Zafar S, Zafar A (2019) Biosynthesis and characterization of silver nanoparticles using *Phoenix dactylifera* fruits extract and their in vitro antimicrobial and cytotoxic effects. *Open Biotechnol J* 13:37–46. <https://doi.org/10.2174/1874070701913010037>
- Zia F, Ghafoor N, Iqbal M, Mehboob S (2016) Green synthesis and characterization of silver nanoparticles using *Cydonia oblong* seed extract. *Appl Nanosci* 6:1023–1029. <https://doi.org/10.1007/s13204-016-0517-z>

